Hindawi Publishing Corporation
Journal of Nanomaterials
Volume 2006, Article ID 63608, Pages 1–5
DOI 10.1155/JNM/2006/63608

# Nonlinear Optical Study of Nano-Sized Effects in a-Si : H Thin Films Deposited by RF-Glow Discharge

**J. Ebothé,[1] K. J. Plucinski,[2] K. Nouneh,[3] P. Roca i Cabarrocas,[4] and I. V. Kityk[5]**

[1] *Laboratoire de Microscopies and d'Etude de Nanostructures, Equipe d'Accueil N3799, BP 138, Universite de Reims, 21 rue Clément Ader, 51685 Reims Cedex 02, France*
[2] *Electronic Department, MUT University, ul.Kaliskiego 2, 00-908 Warsaw, Poland*
[3] *Laboratoire GES 2M, Univesite de Montpellier, 34095 Montpellier, France*
[4] *Laboratoire de Physique des Interfaces et des Couches Minces (CNRS UMR 7647), Ecole Polytechnique, route de Saclay, 91128 Palaiseau Cedex, France*
[5] *Institute of Physics, J. Dlugosz University of Czestochowa, Al. Armii Krajowej 13/15, 42-201 Czestochowa, Poland*

Received 22 August 2005; Revised 14 June 2006; Accepted 13 November 2006

We have evidenced the high sensitivity of infrared-induced second harmonic generation (IR-ISHG) to the structural changes occurred in amorphous hydrogenated silicon films (a-Si : H) prepared by RF-glow discharge technique at different substrate temperatures and doping types. In every case, a maximal signal of the IR-induced SHG is achieved at temperature of about 110 K and pump-probe delaying time about 22–39 ps. It indicates a marked effect of doped subsystems in the observed nonlinear optical effects. A substantial effect of doping is established from a drastic change of the IR-induced SHG behavior presenting an anomaly at about 400 MW/cm$^2$ for a pumping power with wavelength 1.54 $\mu$m. A minimum of the SHG is observed in that case for standard nondoped films. Note here that the doping type does not affect the behavior of the second-order nonlinear optical susceptibility. The thermo annealing leads to a slight decrease of the effective second-order susceptibilities. Larger changes are observed with doped samples for the pump-probe delaying time from about 39 till 24 ps.



## 1. INTRODUCTION

Amorphous hydrogenated silicon (a-Si : H) films are promising optoelectronic materials used as solar cell or other optoelectronic devices requiring additional investigations for a rigorous control of defects in the subsystems formed. These defects are crucially dependent on the method used and the conditions applied in the sample elaboration. In [1, 2], dealing with films obtained by RF glow discharge, it is shown that the decrease of substrate temperature below 200°C reduces the defect concentration. Moreover, the reduction observed elsewhere below 100°C [3, 4] has been explained either by the decrease of the deposition rate giving enough time to manifold precursors $SiH_3$ radicals to find the most favorable sites for incorporation into the film [5] or by the reduction of the polymerization process [6]. Another important aspect to be considered is the film's doping. For that purpose, a very close relationship between the film's microstructure and the degree of doping is reported in [7]. Following ellipsometry measurements, we have established that the imaginary part of the dielectric susceptibility is affected by the doping (*n*- or *p*-type) conditions. However, the results obtained from dc-conductivity and IR spectra cannot provide information concerning the hyperfine influence of the trapping levels formed by interfaces.

From this point of view, nonlinear optical methods and particularly the second-order ones seem to be more appropriate due to their high sensitivity to the low charge density redistribution of disordered materials [8]. Second-order nonlinear methods are forbidden in disordered media and it is necessary to have an additional external field to create long-range ordered alignment. This one could be an electric field, an optical, or a transverse acoustical one [9]. Several works exist now on the nonlinear optical properties of silicon, particularly those devoted to the two-photon absorption spectroscopy [10] and optical second-order harmonic generation in nanocrystallites (NC) [11]. The investigations on the stress/strain effects in silicon wafers grown on insulating substrates by optical second-order harmonic generation (SHG) are also proposed [12].

Recently, these effects have been ascribed to NC incorporated into polycrystalline films. Following the currently

adopted technique, we previously investigated a-Si : H films using an additional induced noncentrosymmetry by means of an external polarized transverse acoustical field [13]. A high sensitivity of the field-induced nonlinear optical method to the silicon films morphology was revealed, which cannot be analyzed by other methods. Therefore, one can expect that the filed-induced optical second harmonic generation may be useful for detection of trapping localized states, which are crucial for transport properties of the material.

Simultaneously, existence of nano-confined effects in large-sized NC possessing long-range ordering is already well known [14]. Nano-confined effects are mainly observed at the borders separating the nanoparticles and the surrounding substrate background. The grain-background interfaces of nanometer sizes can serve as a source of nano-confined quantized levels that could contribute to transition dipole moments determining the hyperpolarizabilities affecting the nonlinear optical effects. In [13], we have shown that an appropriately noncentrosymmetry stimulation of electrons by an external acoustical field could induce substantial noncentrosymmetric charge density distribution. For that purpose, the crucial role of the micro grain size in the observed effects was revealed. Applying an approach introduced for large-sized NC, one can expect a similar influence in the nanosheets (about several nm) separating the grains and their surrounding background. Previously performed molecular dynamics simulations have shown that the phase is formed at the borders separating the grains and background that are slightly different from the remaining background [8].

## 2. EXPERIMENTAL METHODS

### 2.1. Film deposition procedure

The investigated a-Si : H films were prepared by standard RF glow discharge on high optical quality CORNING glass substrates as described in [15]. We have varied several parameters. For the first group of the samples, we have varied substrate temperature and for the second one we have done *n*- and *p*-type doping. Two standard a-Si : H films, indicated by **S1** and **S2** were prepared (under standard conditions), that is, the dissociation of pure silane (10 sccm) at 40 mTorr under the RF power of 1 Watt and substrate temperature of 150 and 300°C, respectively. Three other samples were prepared at 50°C from the dissociation of 4% silane in hydrogen mixtures under a total pressure of 60 mTorr and an RF power of 1 Watt. Sample **S3** was intrinsic while phosphine was added to the mixture to obtain an *n*-type material (sample **S4**) and trymethylboron to obtain *p*-type a-Si : H film (sample **S5**). A synoptic view of the different investigated samples is proposed in Table 1.

Table 1: Labeling and the deposition conditions applied for the different investigated samples.

| Samples labeling | **S1** standard | **S2** standard | **S3** intrinsic | **S4** intrinsic | **S5** intrinsic |
|---|---|---|---|---|---|
| Deposition temperature $T_s$ (°C) | 150 | 300 | 50 (undoped) | 50 (*n*-type) | 50 (*p*-type) |
| Deposition pressure $P$ (mTorr) | 40 | 40 | 60 | 60 | 60 |

### 2.2. Nonlinear optical setup

As a fundamental (probing) laser for the second harmonic generation, we have used pulsed 40 ps Q-switched Gd:YAG laser (presenting traditional Nd:YAG laser with the Gd-containing optical parametrical generator) operating at wavelength 1.76 $\mu$m, with pulse frequency repetition about 3 Hz (see Figure 1). Using parametrical generator from ZnSeTe single crystals cut under appropriate angles, we have obtained 16.0–17.5 ps durated laser pulses operating at 3.7 $\mu$m. The laser power density originated from the optical parametrical generator was varied within the 0.06–0.2 GW/cm$^2$. For the photoinducing changes, we have applied 20 ps Er-glass pulsed laser at $\lambda = 1.54\,\mu$m with pump power density continuously varying up to 1.2 GW/cm$^2$. Using a set of polarizers, we were able to operate by polarization of the incident and output laser beams. The delaying line DL allowed to operate continuously by delayed time between the pumping and probing laser beams. The grating monochromator allowed achieving the doubled frequency output SHG signal that was used for detection of the second-order optical susceptibility by a method described in [16]. The setup allowed the determination of second-order susceptibilities with a precision up to 0.1 pm/V.

## 3. RESULTS AND DISCUSSION

Figure 2 demonstrates a substantial difference of the SHG photoinduced behavior between the doped samples (**S4** and **S5**) and the undoped ones (**S1**, **S2**, and **S3**). In fact, the latter specimens show a substantial enhancement of SHG with the increase of photoinduced field from 0 up to 500 MW/cm$^2$.

Dependence of the effective second-order susceptibility $d_{eff}$ versus the pump-probe delaying times is given in Figure 3 for doped and undoped samples. One can see that there exists a maximum of the second-order optical susceptibility at the pump-probe delaying times in the time interval 15 ps–42 ps. It clearly appears in this case that doped samples (**S5**) exhibit a sharper and higher response, their maximal position occurring at 23 ps instead of 39 ps of the undoped one (**S3**). Besides, the role of deposition temperature on the SHG behavior of a-Si : H films is evidenced in Figure 4 through the study of the second-order susceptibility. Sample **S3** deposited at 50°C exhibits a higher response than **S1** obtained at 150°C. Their particular maximum nonlinear optical (NLO) signals appear at about 120 K.

Such behaviors can be explained only within a frame of electric field induced SHG. These interactions stimulate additional noncentrosymmetry charge density, which is defined by the trapping level's number due to the dopant and the neighboring electron-phonon levels. At the same time, one

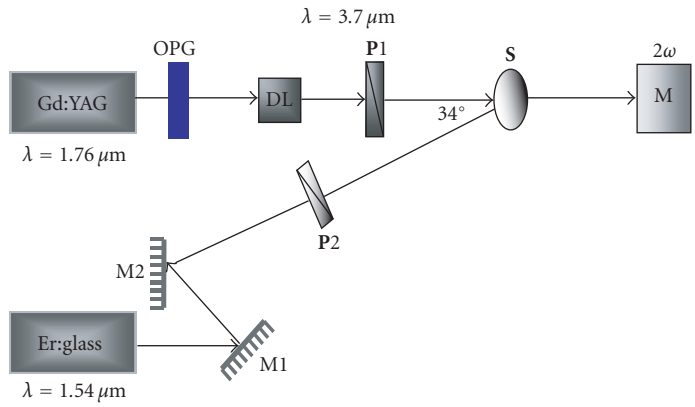


Figure 1: Principal experimental setup for the measurement of IR-induced SHG. All explanations on the process used are given in the text.

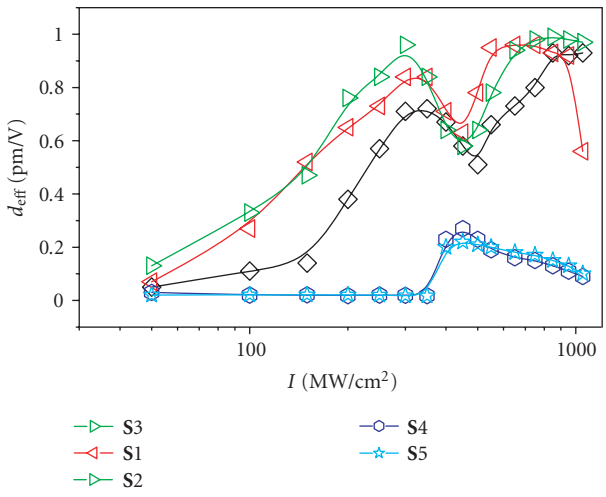


Figure 2: Photoinduced dependence of the efficient second-order susceptibility at fundamental wavelength 3.7 $\mu$m. The data are collected at optimal delaying time of every sample 20–30 ps, each of them being parallel to the polarization direction of the fundamental and pumping beam.

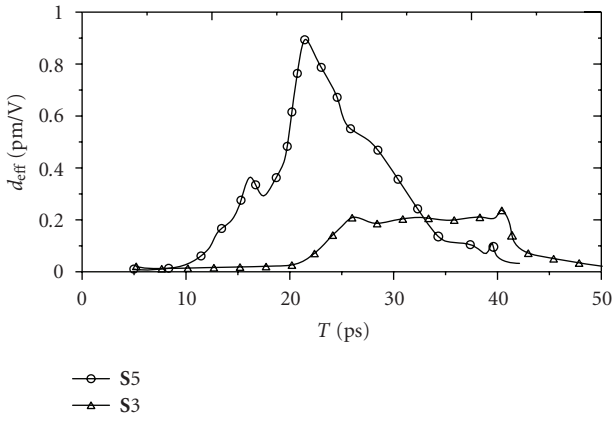


Figure 3: Typical pump-probe delaying dependence. The measurements are performed at 120 K.

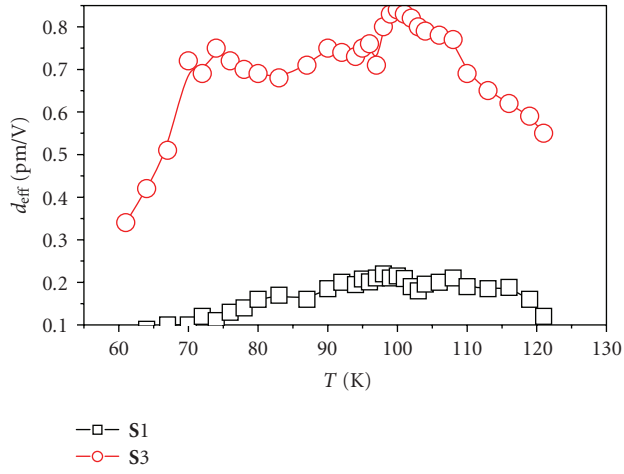


Figure 4: Temperature dependence of the efficient second-order susceptibility at optimal pump-probe delaying time.

can see in Figure 2 that the increase of substrate temperature leads to a slight decrease of the corresponding SHG dependence. This could reflect a decrease of trapping levels at the substrate-film interface. In addition, it appears that doping of $p$- or $n$-type gives almost the same behavior of the photoinduced SHG. This one indicates on a fact that origin of the doping (electrons or holes) do not change sufficiently transitions dipole moments determining corresponding hyperpolarizabilities and susceptibilities, which will be a subject of separate theoretical work in a future. One can therefore conclude that photoinduced nonlinear optics is more sensitive to the total number of the localized levels, contrary to the usual linear elipsometric measurements.

Another result reported in Figure 2 consists in an almost same value of photoinducing pump power at which exist minima and maxima of the second-order susceptibilities $d_{eff}$ for the all investigated samples.

To have a physical insight of these results, a pump-probe NLO relaxation study of the samples has been performed.

From Figure 3, a marked increase of $d_{eff}$ for the doped samples with respect to the undoped samples is clearly shown. This increase is almost two times larger than that of doped samples in the pump-probe range 20–39 ps. Considering the typical times for electron-phonon relaxation together with contribution of electron-phonon subsystems, one can expect an occurrence of additional IR-induced phonon mechanisms for hole and electron carriers which is quite different from that of subsystems of electron-phonon levels determining the photoinduced processes. The as-reported results appear only during the excitation and disappear out for the temperature region of about 110 K. It is necessary to emphasize that the observed second harmonic generation exists only during the photoinducing beam and completely disappears after its removement.

The observed effect is optimal at temperature range 80–120 K. There exists also a probability of an appearance a slightly modified structural phases at the borders separating the silicon films and the surrounding background. Our use of molecular dynamics simulations for the study of isostructural SiON films deposited on silicon [17] showed that for both sides of the interface there occurs a thin layer which can create a nanosheet with partial crystallization. Due to the thinner sheet, its structural control is possible only by photoinduced SHG.

By and large, it is assumed for nanocrystallites that two factors are responsible for this size-dependent SHG response: the size distribution of crystallites in film and the size distribution in a single crystallite due to random shape distortions [17]. In the case of amorphous-like films with partially nonhomogenous structure, nanoparticles could play the role of interface structure between the morphological grains and the background. It can be assumed that SHG is a result of the direct-gap $\Gamma_{15}$–$\Gamma_{25'}$ transitions in silicon nanocrystallites. Although the photon energy is less than the resonance value ($\sim$3.3 eV) for bulk silicon, the resonant SHG is achieved due to the band tail—band tail transition. The broadband tails inside the band gap of nanoparticles mainly consist of defect states that are created due to grain boundary defects. The exponential slope constants of band tails can be evaluated in 300–650 meV range. Therefore, the tail-to-tail transitions may be the possible reason of SHG response [18].

## 4. CONCLUSION

Following the performed photoinducing optical second harmonic generation, we have discovered a high sensitivity of SHG to the structural modifications occurred in hydrogenated silicon amorphous-like films due to some changes in their deposition conditions and doping. Considering the typical times for electron-phonon relaxation together with contribution of electron-phonon subsystems, one can expect an occurrence of additional IR-induced phonons which is quite different from that of subsystems of electron-phonon levels determining the photoinduced processes. We have found that the doping of the films leads to drastic changes of the IR-induced behavior of the SHG, possessing an anomaly for a pumping power of 1.54 $\mu$m at about 390 MW/cm$^2$, which becomes a minimum for the standard nondoped films. The thermo annealing leads to a slight decrease of the effective second-order susceptibilities. Larger changes are observed for the pump-probe dependences, particularly for the doped films. We observed in that case a decrease of the pump-probe delaying time from about 38 ps up to 25 ps. It is necessary to emphasize that the type of the doping does not influence substantially on the behavior of the second-order nonlinear optical susceptibility. It appears that doping of *p*- or *n*-type gives almost the same behavior of the photoinduced SHG. This one reflects a fact that origin of the doping (electrons or holes) does not change substantially transition dipole moments determining corresponding second-order hyperpolarizabilities and susceptibilities.

## REFERENCES


[1] M. Kunst and H.-C. Neitzert, "The influence of deposition temperature and annealing temperature on the optoelectronic properties of hydrogenated amorphous silicon films," *Journal of Applied Physics*, vol. 69, no. 12, pp. 8320–8328, 1991.

[2] P. Roca i Cabarrocas, Z. Djebbour, J. P. Kleider, et al., "Hydrogen, microstructure and defect density in hydrogenated amorphous silicon," *Journal de Physique I*, vol. 2, pp. 1979–1998, 1992.

[3] Y. Hishikawa, S. Tsuge, N. Nakamura, S. Tsuda, S. Nakano, and Y. Kuwano, "Device-quality wide-gap hydrogenated amorphous silicon films deposited by plasma chemical vapor deposition at low substrate temperatures," *Journal of Applied Physics*, vol. 69, no. 1, pp. 508–510, 1991.

[4] M. K. Cheung and M. A. Petrich, "$^{29}$Si magnetic resonance study of amorphous hydrogenated silicon plasma deposited at 50°C," *Journal of Applied Physics*, vol. 73, no. 7, pp. 3237–3241, 1993.

[5] T. Kamei, G. Ganguly, N. Hata, and A. Matsuda, "Defect determination kinetics during the growth of a-Si:H," *Journal of Non-Crystalline Solids*, vol. 164–166, part 1, pp. 43–46, 1993.

[6] P. Roca i Cabarrocas, "Towards high deposition rates of a-Si:H: the limiting factors," *Journal of Non-Crystalline Solids*, vol. 164–166, part 1, pp. 37–42, 1993.

[7] P. Roca i Cabarrocas, "Deposition of intrinsic, phosphorus-doped, and boron-doped hydrogenated amorphous silicon films at 50°C," *Applied Physics Letters*, vol. 65, no. 13, pp. 1674–1676, 1994.

[8] O. Ostroverkhova, A. Stickrath, and K. D. Singer, "Electric field-induced second harmonic generation studies of chromophore orientational dynamics in photorefractive polymers," *Journal of Applied Physics*, vol. 91, no. 12, pp. 9481–9486, 2002.

[9] W. Gruhn, I. V. Kityk, and S. Benet, "Photoinduced optical second harmonic generation in Fe-Co metallic spin glasses," *Materials Letters*, vol. 55, no. 3, pp. 158–164, 2002.

[10] D. H. Reitze, T. R. Zhang, W. M. Wood, and M. Downer, "Two-photon spectroscopy of silicon using femtosecond pulses at above-gap frequencies," *Journal of the Optical Society of America B*, vol. 7, no. 1, pp. 84–89, 1990.

[11] D. E. Milovzorov, A. M. Ali, T. Inokuma, Y. Kurata, T. Suzuki, and S. Hasegawa, "Optical properties of silicon nanocrystallites in polycrystalline silicon films prepared at low temperature by plasma-enhanced chemical vapor deposition," *Thin Solid Films*, vol. 382, no. 1-2, pp. 47–55, 2001.

[12] Y. Gu, C. Hu, L.-J. Cheng, D. Y. Zang, and G.-P. Li, "Investigation of stress/strain of silicon on insulator using optical second harmonic generation method," in *Optical Characterization Techniques for High-Performance Microelectronic Device Manufacturing*, vol. 2337 of *Proceedings of SPIE*, pp. 93–102, Austin, Tex, USA, October 1994.

[13] J. Ebothé, I. V. Kityk, P. Roca i Cabarrocas, C. Godet, and B. Equer, "Acoustically induced optical second harmonic generation in hydrogenated amorphous silicon films," *Journal of Physics D: Applied Physics*, vol. 36, no. 6, pp. 713–718, 2003.

[14] K. J. Pluciński, I. V. Kityk, J. Kasperczyk, and B. Sahraoui, "The structure and electronic properties of silicon oxynitride gate dielectrics," *Semiconductor Science and Technology*, vol. 16, no. 6, pp. 467–470, 2001.

[15] P. Roca i Cborrocas, J. B. Chévrier, J. Huc, A. Lloret, J. Y. Parey, and J. P. M. Schmitt, "A fully automated hot-wall multiplasma-monochamber reactor for thin film deposition," *Journal of Vacuum Science & Technology A: Vacuum, Surfaces, and Films*, vol. 9, no. 4, pp. 2331–2341, 1991.

[16] I. V. Kityk, B. Marciniak, and A. Mefleh, "Photoinduced second harmonic generation in molecular crystals caused by defects," *Journal of Physics D: Applied Physics*, vol. 34, no. 1, pp. 1–4, 2001.

[17] D. Milovzorov and T. Suzuki, "Size-dependent second-harmonic generation by nanocrystals prepared by plasma-enhanced chemical-vapor deposition," *Applied Physics Letters*, vol. 75, no. 26, pp. 4103–4105, 1999.

[18] O. A. Aktsipetrov, P. V. Elytin, A. A. Nikulin, and E. A. Ostrovskaya, "Size effects in optical second-harmonic generation by metallic nanocrystals and semiconductor quantum dots: the role of quantum chaotic dynamics," *Physical Review B*, vol. 51, no. 24, pp. 17591–17599, 1995.